Ben Richard Hughes, Mak Cheuk-Ming, A study of wind and buoyancy driven flows through commercial wind towers, Energy and Buildings, Volume 43, Issue 7, July 2011, Pages 1784-1791, ISSN 0378-7788, http://dx.doi.org/10.1016/j.enbuild.2011.03.022

A Study of Wind and Buoyancy Driven Flows Through Commercial Wind Towers

Dr Ben Richard Hughes
Dubai Energy Research Group, Heriot-Watt University. Academic City Dubai.

Dr Mak Cheuk-ming
Department of Building Services Engineering, The Hong Kong Polytechnic University, Hung Hom, Kowloon, Hong Kong.

Abstract

Commercial wind towers have been the focus of intensive research in terms of their design and performance. There are two main forces which drive the flow through these devices, external wind and buoyancy due to temperature difference. This study examines the relationship between these two forces and the indoor ventilation rate achieved. The work uses Computational Fluid Dynamics (CFD) Modeling to isolate and investigate the two forces and draw comparisons. The study found that as expected the external driving wind is the primary driving force providing 76% more internal ventilation than buoyancy driven flow, which is deemed secondary. Moreover the study found that the effect of buoyancy is insignificant without an external airflow passage other than the wind tower itself. The addition of an external airflow passage such as a window in combination with buoyancy force increased the indoor ventilation by 47%. Therefore the careful positioning of windows in conjunction with internal heat source has the potential to overcome the lack of external wind driven forces in dense urban environments.

Keywords: Wind Tower, CFD, Buoyancy, Urban Environment, Indoor Ventilation.

1.0 Introduction

According to the World Business Council for Sustainable Development (WBCSD), buildings account for up to 40% of the worlds energy use [1]. Breaking down the energy consumption of buildings reveals that Heating, Ventilation and Air Conditioning (HVAC) systems account for up to 60% of domestic buildings energy consumption [2]. This represents a significant opportunity for reducing the buildings energy consumption and carbon footprint.

There are two methods of ventilating occupied spaces. Namely, natural ventilation and mechanical ventilation. Mechanical ventilation techniques use equipment to induce or move conditioned airflow. Typical examples of mechanical ventilation are fans and HVAC units. Typical examples of natural ventilation are building openings like windows and doors. Thus natural ventilation refers to outdoor air supply (macro-climate) to indoor (micro-climate) through non-mechanical methods.

The British Standards Institution (BSI) has devised a code of practice for supplying fresh air via non-mechanical means to ensure that this approach is not to the detriment of the building's occupants [3]. Non-mechanical methods are commonly employed in buildings by strategic positioning of openings to allow fresh air to enter and the inclusion of air bricks and roof vents to allow the stale air to exhaust.

Currently, designers and engineers have incorporated traditional architectural passive ventilation solutions into new and existing buildings. The application of modern engineering methods such as Computational Fluid Dynamics (CFD) to analyse and optimise solutions has developed a new generation of Eco-technologies to meet the energy demands of the future.

An example of one such Eco-technology is the wind tower (Or wind catcher/ wind vent). Based on traditional Middle Eastern Malgalf, these device channel external air at a high velocity to service ground level accommodation using no mechanical intervention.

A wind tower has been subject to extensive investigation and optimisation using CFD and full scale experimental testing [4]. Commercial wind vents are divided into quadrants, which allow fresh air to enter as well as stale (used) air to escape irrespective of the prevailing wind direction, shown in Figure 1.

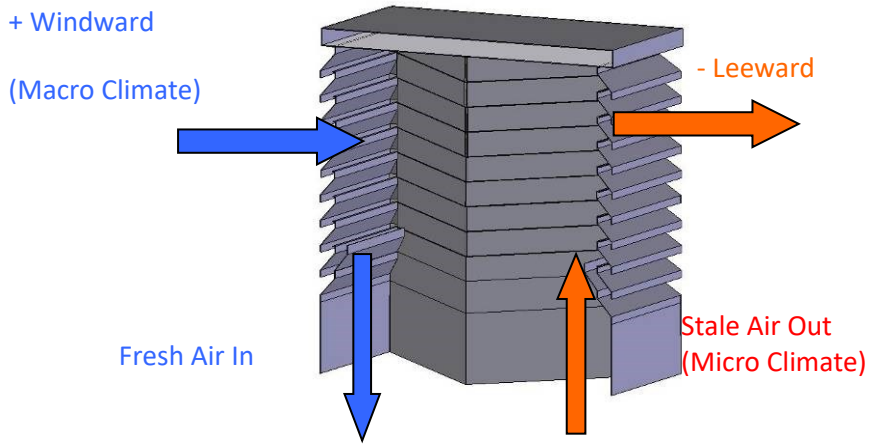

Figure 1 Cross Section of a Commercial Wind Tower

There are two driving forces for the wind vent. The primary force provides fresh air driven by the positive air pressure on windward side, exhausting stale air with the assistance of the suction pressure on the leeward side

The secondary force is temperature driven and termed "the stack effect". The density of air decreases as its temperature increases causing layers of air to be stacked. The internal and external temperature difference (micro to macro climate) drives the airflow through the ventilator. If the external temperature is lower than the internal temperature, then the buoyancy of the warmer air causes it to rise and exhaust through the unit.

This study investigates the two driving forces for the wind tower and evaluates each contribution to the ventilation rates achievable. The forces are considered in isolation using CFD modeling and validated using wind tunnel experimentation. The forces are then combined using CFD modeling and validated using full scale experimental testing in the natural environment. Thus the driving forces are fully evaluated both in simulated scenario and the actual natural environment, to allow a comprehensive evaluation of the devices effectiveness as a low carbon alternative to traditional natural ventilation techniques.

2.0 Previous Related Work

Hunt and Linden, [5], used experimental and theoretical investigations to analyse the fluid mechanics of natural ventilation-displacement by buoyancy-driven flows. A major result of this work was the identification of the form of the non-linear relationship between the buoyancy and wind effects. The study showed that there is a Pythagorean relationship between the combined buoyancy and wind-driven velocity. The velocities which are produced by buoyancy and wind forces act in isolation. This relationship enables the prediction of airflow capabilities in buildings using natural ventilation.

Parker and Teekaram, [6], produced a guide to wind driven natural ventilation systems. This work was carried out by the Building Services Research and Information Association (BSRIA). The guide presents a methodology for sizing wind vent devices for the application of building ventilation. The formulae are based on the British standard BS5925:1991. In the BSRIA guide, additional mathematical formulae are presented for building characteristics such as heat gains and air leakage. The formulae use assumed values for the pressure distribution, and are applied in isolation to combat heat gain and air leakage. Although the guide presents a series of case studies, the mathematical formulae are not evaluated and no indication is given as to the accuracy of the results.

Elmualim, [7], investigated the use of mathematical equations proposed by BS5925:1991 for the application of a wind vent device. The mathematical equations were evaluated against experimental testing in a seminar room in the University of Reading UK. The wind vent was also evaluated against the use of a standard openable window. The window and wind vent had equivalent opening areas to determine the advantage over traditional natural ventilation techniques. The results of the experimental testing showed the mathematical formula consistently over-estimated the ventilation rate. The author also concluded that the wind vent device provided a substantially greater ventilation rate than an equivalent area of openable window.

Elmualim, [8], used CFD modelling to evaluate the performance of a wind vent device and compared the results to wind tunnel experimentation. The study constructed a computational model of a commercial wind vent device. The louver sections were reduced to porous flat surfaces - due to the complexity of the geometry - with an orifice flow calculation used in the solver to represent resistance to air flow. In addition the damper and diffuser sections were omitted - for the same reason - no compensating calculation was used in the solver.

Liu and Mak [9], used CFD to investigate the ventilation capabilities of a wind vent system connected to a room. The study used louver geometry but omitted the damper and diffuser sections. The computational model was run for external wind speeds of the range 0.5 - 6 m/s. The results were compared to previous published wind tunnel results. The results of this numerical work showed that the CFD predictions correlate with the

wind tunnel testing results. This work demonstrated the predictive capabilities of CFD for wind vent applications.

Hughes and Ghani, [10], used CFD to investigate the capability of a wind vent device to meet the British Standards (BS5925:1991). The investigation simulated a current commercially available wind vent installed in a classroom. The full geometry of the wind went was recreated including louvers and dampers. The CFD results of this investigation showed that the wind vent device met the British standard recommendations. At low levels of external wind - regardless of wind direction - the device is capable of meeting BSI standards. This investigation used the standard k-e simulation model. The work demonstrated the effectiveness of this technique for predicting airflows through the device.

Hughes and Ghani, [11], used CFD to investigate the effect of the control dampers from a wind vent on the indoor air distribution. The purpose of this study was to ascertain an operating range for the control dampers; to deliver the maximum internal air movement rate. A total of 19 CFD models were created using the full geometry of the wind vent device installed in a classroom, with the damper angle varied in each case by five degrees. The CFD results showed that the optimum operating range for the control dampers was in the region of 45 - 55°. To quantify the validity of these computational results, the authors compared them to previous published CFD and experimental work. Good correlation between both sets of data validated the CFD work.

Hughes and Ghani [12] used CFD to investigate the effect of the external louvre angle of a commercial wind vent to the delivered ventilation rate into the occupied space. This work considered the external louvre as an airfoil and thus employed a variation in attack angle to evaluate the effect on performance of the device. This work established a relationship between trailing edge stall and ventilation rate, and concluded an optimum external louvre angle of 35° for the device.

Hughes and Ghani [13] used CFD to evaluate the feasibility of a passive-assisted wind vent device. The device combined a low powered solar driven fan inside a commercial wind vent device. The work compared the delivered ventilation flow rates against legislative requirements and concluded a 20Pa fan is sufficient to meet the requirements.

From the previous related work it is evident that the effect of wind tower device have been studied using CFD and wind tunnel testing for validation. Moreover the mathematical prediction methods have been examined by numerous approaches. This study isolates the combined driving forces and examines each using CFD, wind tunnel simulation and full scale experimentation. Thus the contribution of each force to the overall effectiveness of the commercial device is established and presented.

3.0 CFD Modeling

3.1 Wind Driven Simulations

The CFD modeling described in this work was performed using a commercially available software package, namely FLUENT (Processor) and Gambit (pre-processor). The airflow was simulated using the standard k-e model. This technique is well established in the field of natural ventilation research [14,15 and 16].

The governing equations are the Navier-Stokes and Energy equation which will not be repeated here but are available in detail in literature [17].

Gambit was used to create the fluid domain. The domain consist of three zones. The first zone is the Macro climate, or external air, zone 2 is the wind tower, and zone three is the micro climate or ventilated space. The macroclimate represents the external air supply or velocity inlet and also the exhaust from the wind tower or pressure outlet. The limits of the macroclimate for the fluid domain are dependant on the dimensions of the area of the wind tower, to avoid reversed flow or distortion of results the limits were set at 2.5 times the distance of each wall of the wind tower. Additionally the walls of the macro climate were set as symmetry, thus removing any adverse effect from the building geometry.

Zone 2 is the wind tower under investigation. The Wind tower geometry, was a 1000 x 1000 mm Wind tower including cross dividers and damper faces. The Wind tower contained 10 louvers spaced at 50mm between each opening louver (The bottom and top louvers connect the structure and do not allow airflow through). The Wind tower was centrally placed above the micro climate or ventilated space.

Zone 3 is the ventilated space, was determined as a small classroom of 6000 x 6000 x 2500 mm dimensions [18]. The full flow domain is shown in Figure 2.

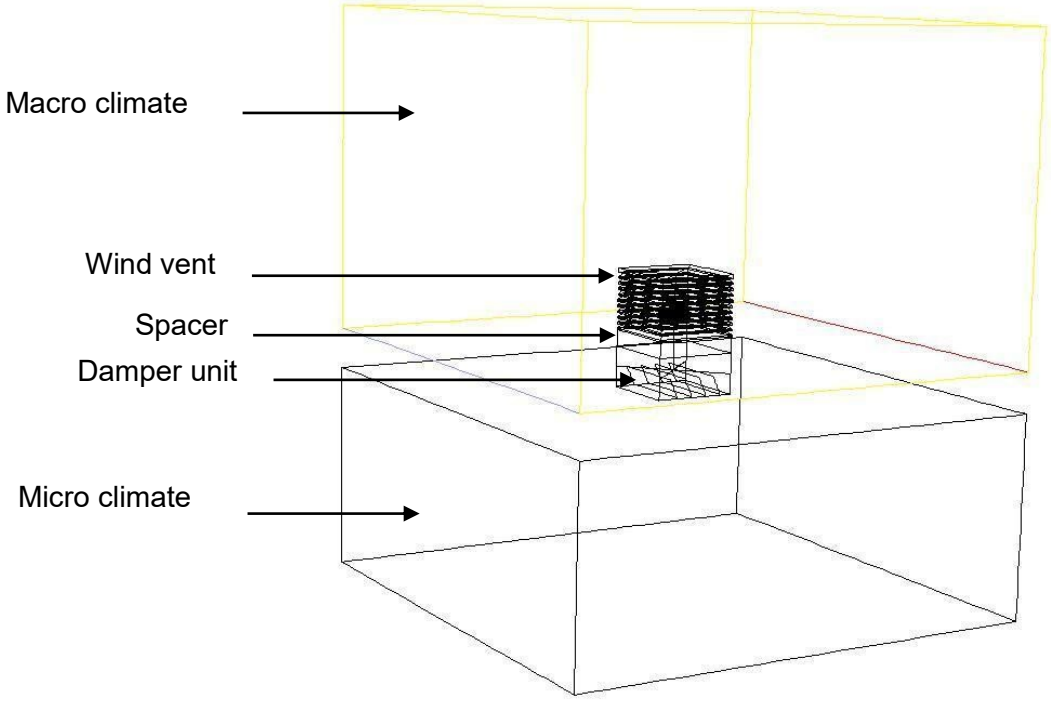

Figure 2 Gambit flow domain representation of the physical geometry under investigation

3.2 Boundary Conditions

Accurate modeling of the louvers geometry is paramount to capture the flow. All geometry created for the micro climate were named as walls. The porous jump model was not used to model the pressure drop created by louvres. Instead, an extensive process of local grid enhancement was carried out on that region. Downstream, as shown in Figure 3, the diffuser or egg crate grill was modeled using the porous jump boundary condition.

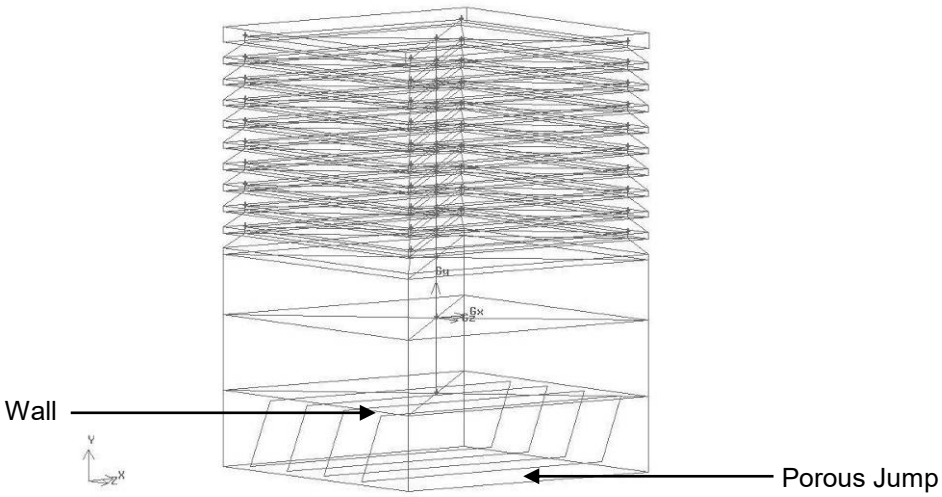

Figure 3 Gambit representation of the wind tower geometry

The porous jump acts as thin membrane or filter with user defined inputs of permeability of 0.91m^2 and medium thickness of 0.01m to replicate the wind tower diffuser. These values are taken form physical measurements of the Wind tower diffuser. A tertiary term of pressure jump coefficient is available to the user for this type of boundary condition, however without sufficient experimental testing a reliable coefficient is currently unavailable, the software reduces to the Darcy's law in the absence of this input [17].

$$\Delta p = -\left(\frac{\mu}{\alpha}v + C_2\frac{1}{2}\rho v^2\right)\Delta m \qquad \textbf{Equation 1}$$

Where:

α	is the permeability of the medium	(m^2)
C_2	is the pressure-jump coefficient	(1/m)
Δp	is the pressure change	(Pa)
μ	is the laminar fluid viscosity	(kg/ms)
Δ m	is the thickness of the medium	(m)
ρ	is the fluid density	(kg/m^3)
υ	is the fluid velocity	(m/s)

The macro climate created, to simulate the incident wind velocity may be seen in figure 2, consists of a velocity inlet at one complete side, and a pressure outlet (atmospheric pressure) on the opposing side. The remainder of the macro climate faces were named as symmetry faces, thus alleviating any return velocities which may distort the results. The incoming and free flow velocities were set as a constant 4.5 m/s, unless otherwise stated in results section. No boundary layer separation was considered at such low velocities.

Grid Verification

The grid adaptive technique used in this investigation was the *hp* method, [19] which requires a refinement using high order approximations, with accuracy measured using a posterior error indicator (defined by the user) between each approximation. The complete computational domain was split and refined in three areas (corresponding to the three fluid volumes): the wind vent and immediate surrounding zone; remaining macro-climate; and finally the micro-climate. The *hp* method required a posteriori error indicator which was defined as the diffuser average area-weighted velocity result. Gambit allows for two types of element node patterns to be selected with increased

number of nodes (*p*-enrichments). The variation of these two types had insignificant effect on the posteriori error indicator. The *h*-refinements were applied to the three areas in three correlating stages shown in figure 4.

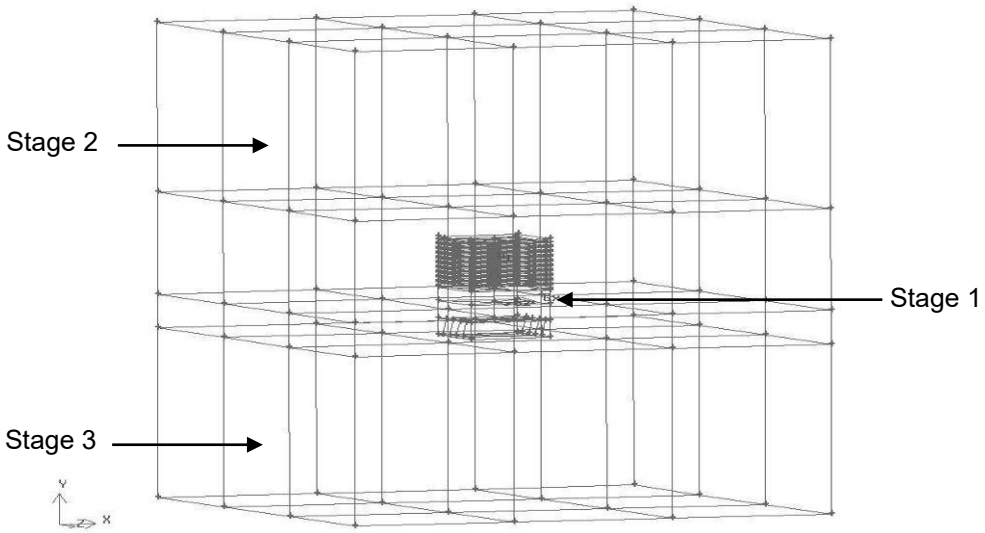

Figure 4 Grid adaption areas identified by stage of adaption

The grid adaption process increased the number of elements by 445,793. Each stage continued until an acceptable compromise was reached between: number of elements; computational time to solve; and the posteriori error indication, as depicted in figure 5.

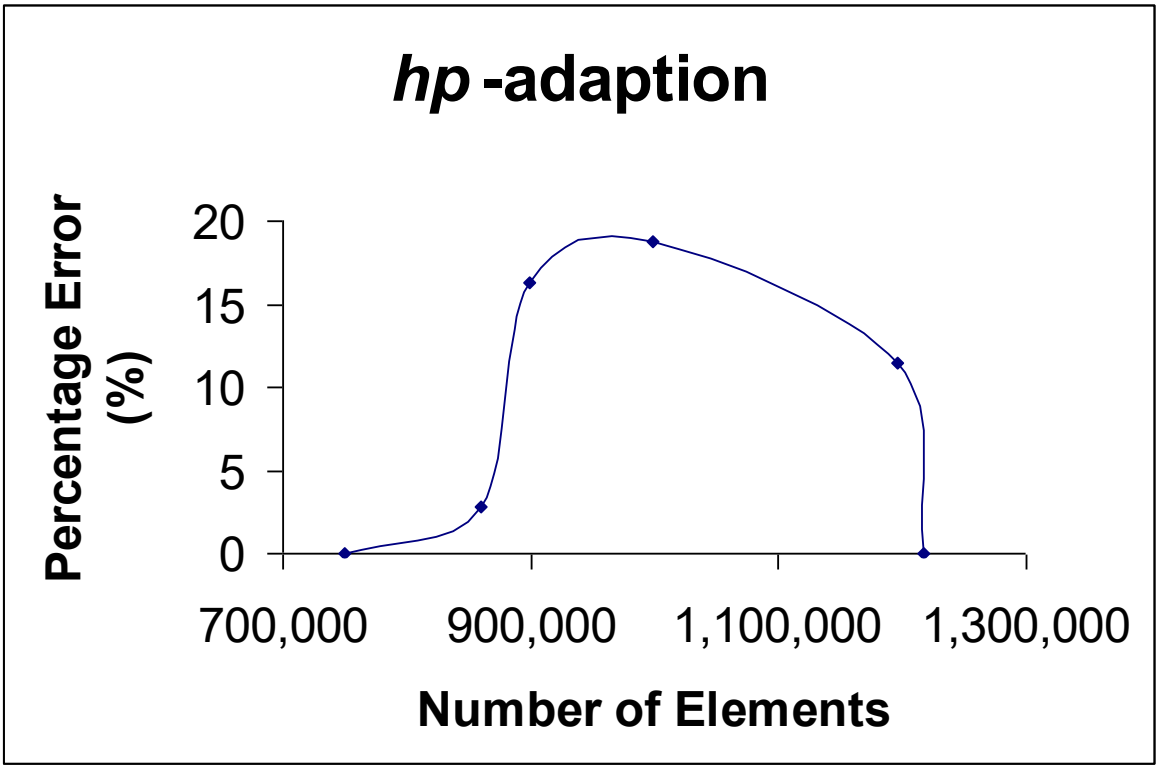

Figure 5 Error reduction through successive *hp*-adaption stages

At 1,196,003 elements the error indication between refinements was at its lowest in the final two stages; coupled with the computational time, made it an acceptable compromise. These node spacing's were applied to each investigation.

3.3 CFD Wind Driven Flow Visualisation

Figure 6 shows the con-current flow entering from the left velocity inlet boundary. The flow splits at the wind vent face with air entering the macro to micro climate interface (wind vent) and the remaining flow passing over and exiting to the right pressure outlet boundary. The geometry shown includes a supplementary vertical plane created to assist in the illustrative analysis of the model.

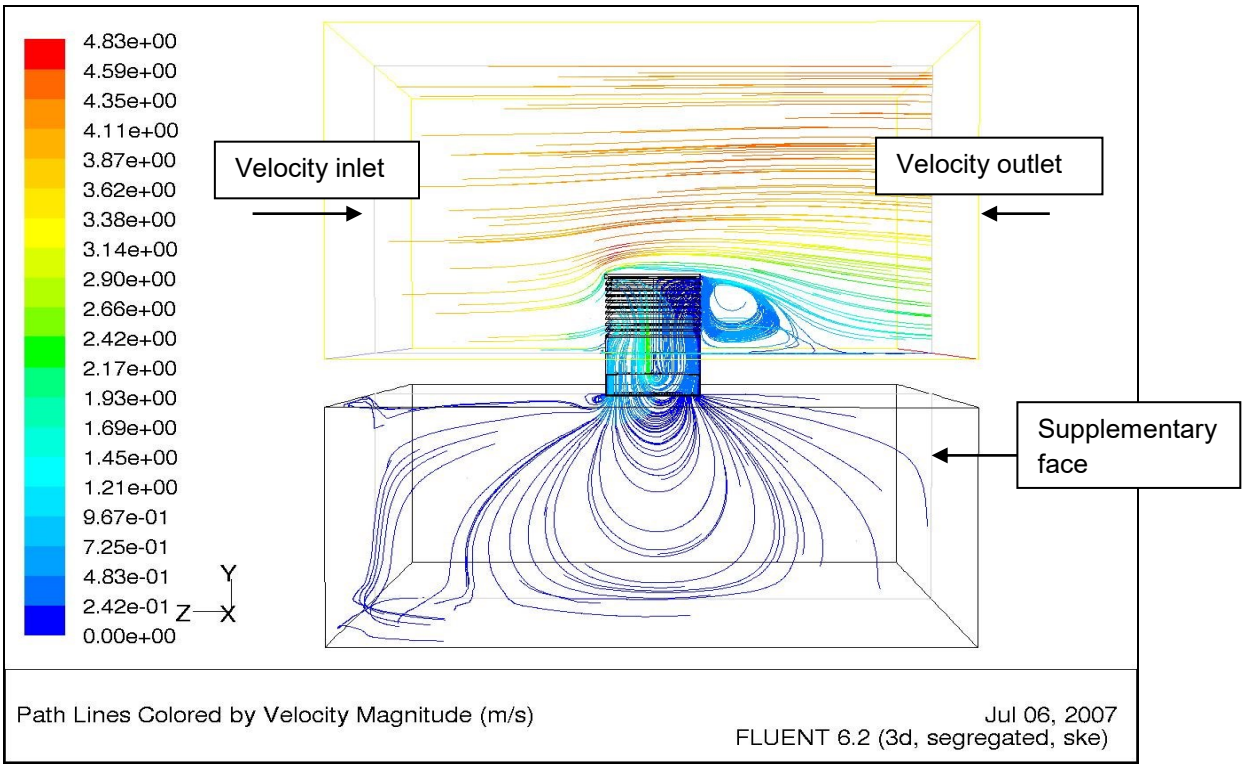

Figure 6 Velocity vectors simulating the con-current flow at 4.5m/s through the wind vent

The velocity contour plot (Figure 7) shows a distinct area of higher velocity directly below the wind vent. This was expected, due to the displacement effect between inlet and outlet, where the air entering the wind catcher produced a positive pressure, a corresponding negative or suction effect is crated drawing the air out of the room through the wind catcher.

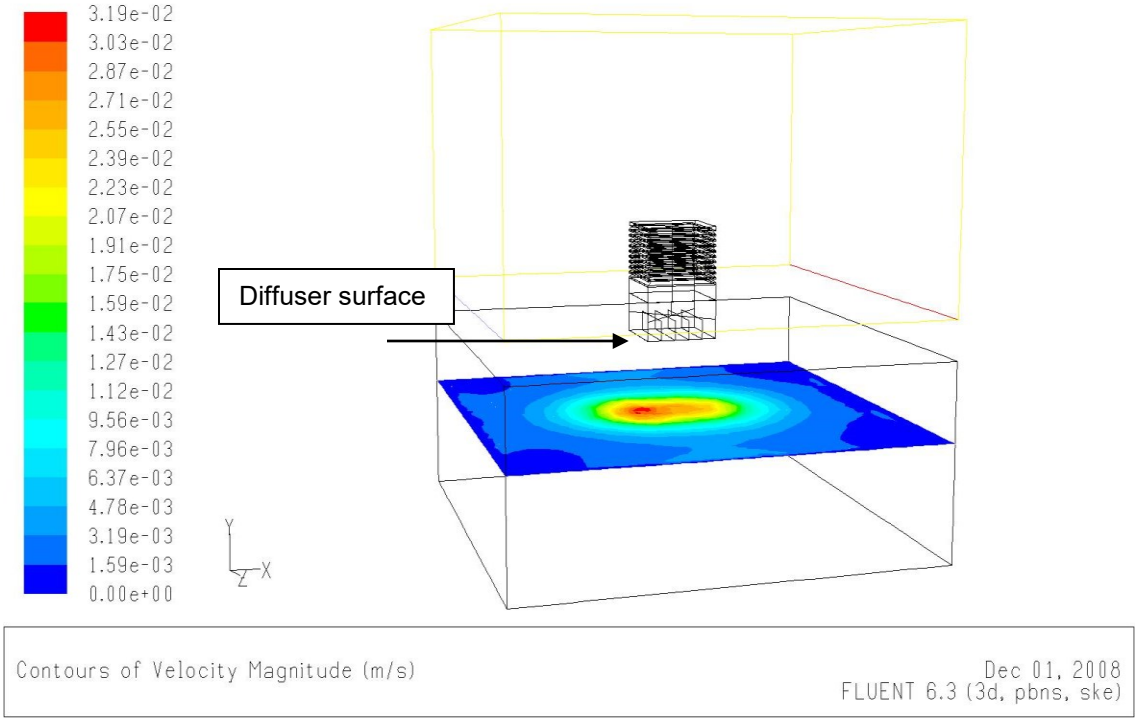

Figure 7 Contour plot of internal velocity at external velocity of 4.5 m/s

4.0 Experimental Model

To verify and validate the CFD modeling, full scale experimental testing was carried out. The macro climate was the natural environment, the wind tower was located in Sheffield Hallam University during 2008, with the occupied space being a standard classroom, as defined in [18]. To facilitate experimental variables, a standard (commercially available) wind vent, was designed and installed. The micro-climate was selected to most accurately reflect the simulation models. The simulation model had room dimensions of 6 x 6 x 2.5 m, with a volume of 90m^3. The experimental test room had a volume of 80m^3, the results were normalized to make accurate comparisons.

The completed assembly of: the top hat; louver section; and cross divider structure, and stood at 1m square as per the CFD model shown in figure 8.

Figure 8 Experimental wind tower in situe

The wind vent was located centrally within the micro-climate. A test grid - marked on the floor - to locate the position of the nine sample points required (in comparison with the simulation model vertex). The position of the sample points was calculated to be evenly distributed within the floor area, (to mimic the vertex distribution within the simulation model). The exact position of the sample points is shown in Figure 9.

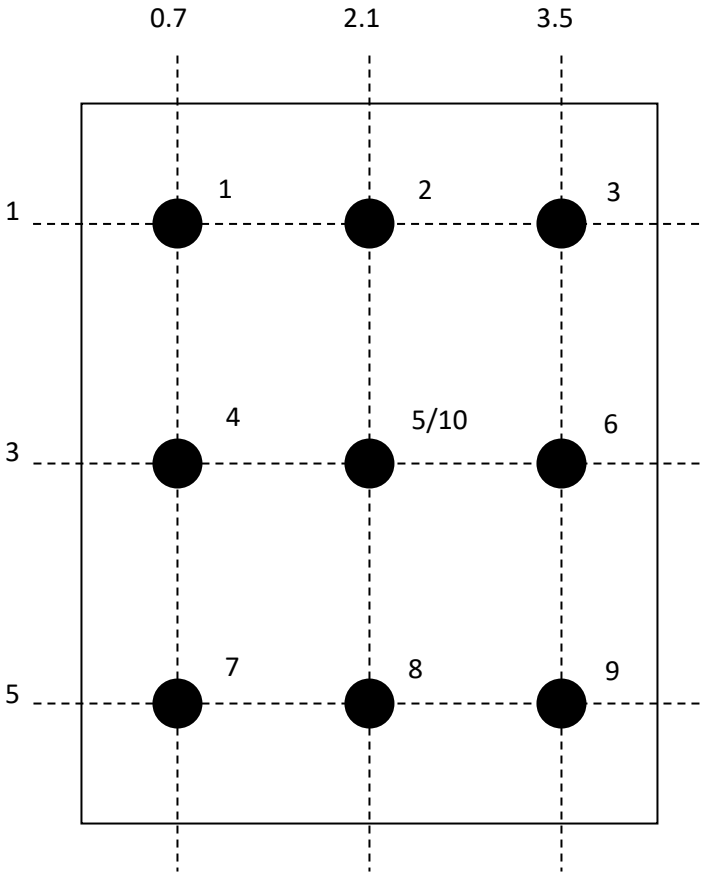

Figure 9 Location of sample points within the micro climate (all dimensions in m)

The centre of the wind vent was located directly above the sample point with coordinates, 2.1, 3. This sample position has two sample points, differentiated by the vertical distance at which the sample was taken. The vertical distance for the nine points was 1.5 m with the additional point taken at 2.75m (diffuser level).

Over a 6 month period each point was sampled daily to provide air velocity readings, using a hot wire thermal velocity probe and meter. These readings were time averaged and correlated to the locally installed weather station, to draw a comparison of internal air movement to external wind velocity shown in figure 10.

Figure 10 Experimental set up of sampling points

4.1 Validation

The CFD simulations must be validated to provide confidence in their accuracy. To validate the CFD simulations the computed results were compared with the experimental data as defined in [20]. A range of external velocities and directions were measure and compared to ensure rigidity in the validation, presented here (Figure 11) is one external velocity. The external velocity and internal velocity were time averaged results (Matched timings) to provide a steady state equivalent full details are available in [21].

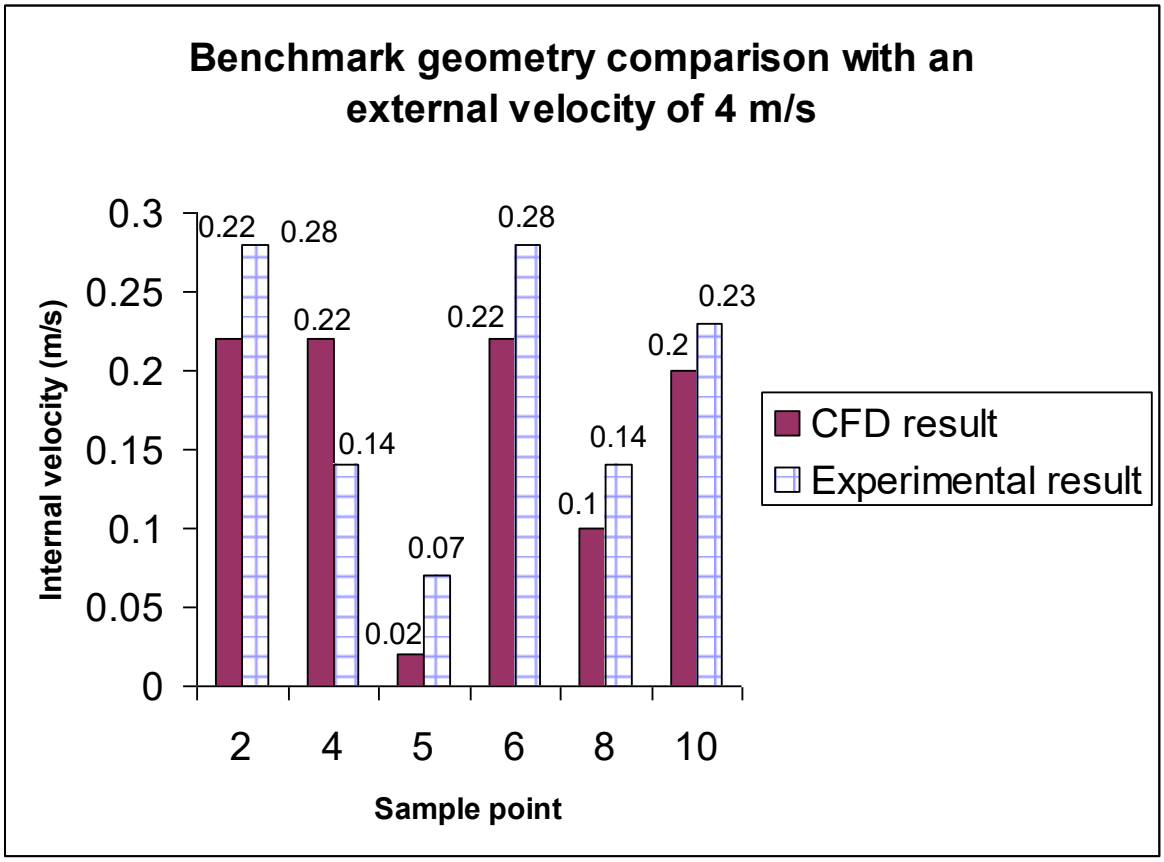

Figure 11 Comparison of CFD and experimental results with external velocity of 4m/s

From figure 11 it is determined that across the sample points there is an error range of 3-8%, but the trend is in agreement with the CFD model underestimating the flow at most sample locations. As the trends are consistent then according to [22] the accuracy is sufficient to validate the model. The validation was compared across numerous external velocities and found to be in agreement, presented here is a representative result.

5.0 CFD Modeling Buoyancy driven simulations

This part of simulation adopted the commercial CFD code FLUENT that is made up of three parts: the pre-processor software GAMBIT, the solver, and the post-processor.

A full scale office of 2.48m (W) ×2.48m (L) ×2.48m (H) [23] was used in CFD modeling to study the wind catcher ventilation performance in relation to thermal conditions. In the office model, the heat sources were the four lightings, two computers and two persons. The heat input of each person was 75W; the heat input of each lighting was 34W; and the heat input of computer one and two was 173W and 108W respectively. The room model was shown in figure 12. A wind catcher of 800mm (L) ×800mm (W) ×1500mm (H), with six louvers was installed at the center of the room roof. The louver projection

length was the same of the gap between two adjacent louvers. The assumed wind speed at 10m above the ground level is 10m/s. The approximate mean velocity profile of the approaching wind was derived from a power-law model. The wind profile in this study is calculated by the following equation (1):

$$U(z) = U_G \times (\frac{z}{z_G})^{0.25} \qquad (1)$$

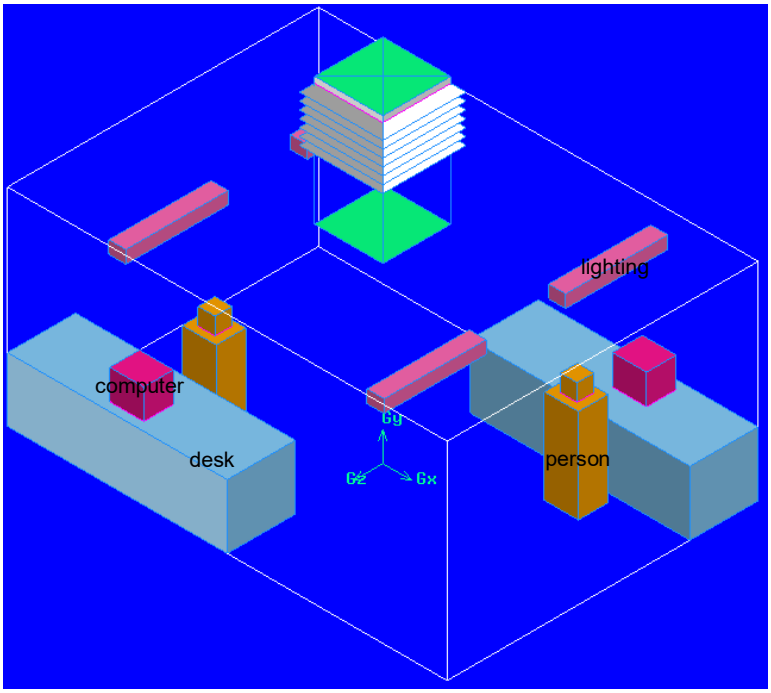

Figure 12 the room model with wind catcher system

Three cases were used to study the buoyancy effect in steady state. Case 1 was a basic case having sources without thermal emission and the room without a window. Case 2 was a case with heat sources and without a window. Case 3 was a case with heat sources and a window in the leeward side of the room.

5.1 Flow visualization of buoyancy driven model

Figure 13 (a) showed the velocity vector of the middle plane in the basic room model. The supply air from the windward quadrant of the wind catcher system reached the floor and then spread along the floor and arose along the walls. The air finally exhausted from the other quadrants. In addition, the high velocity airflows generated in the upright direction from the inlet of wind catcher and the airflows were much uneven in the room. Two vortexes were formed in the leeward of the wind catcher system because of the negative pressure on the leeward side. The velocity vector of the case 2 was shown in figure 13 (b). It could be seen that the vortexes in the leeward side of the wind catcher changed because of the heat sources. The velocity vector of the case 3 was shown in figure 13 (c). When the window was positioned at the leeward side, a little extra wind is induced into the room. The vector condition was basically the same as the figure 11 (b).

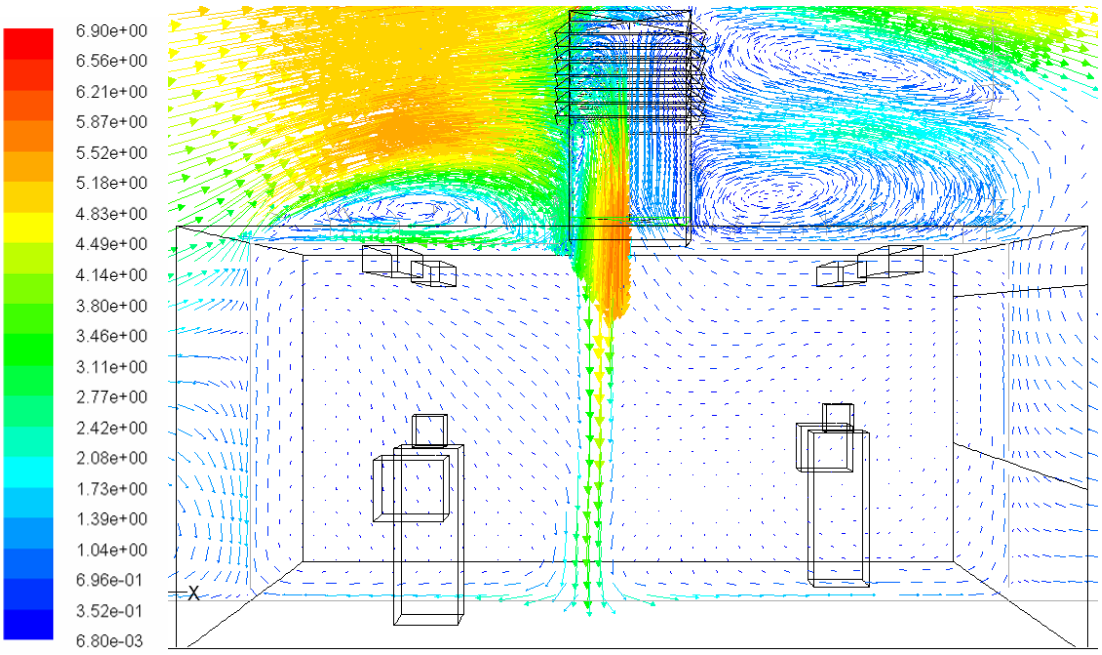
6.90e+00
6.56e+00
6.21e+00
5.87e+00
5.52e+00
5.18e+00
4.83e+00
4.49e+00
4.14e+00
3.80e+00
3.46e+00
3.11e+00
2.77e+00
2.42e+00
2.08e+00
1.73e+00
1.39e+00
1.04e+00
6.96e-01
3.52e-01
6.80e-03
X

(a)

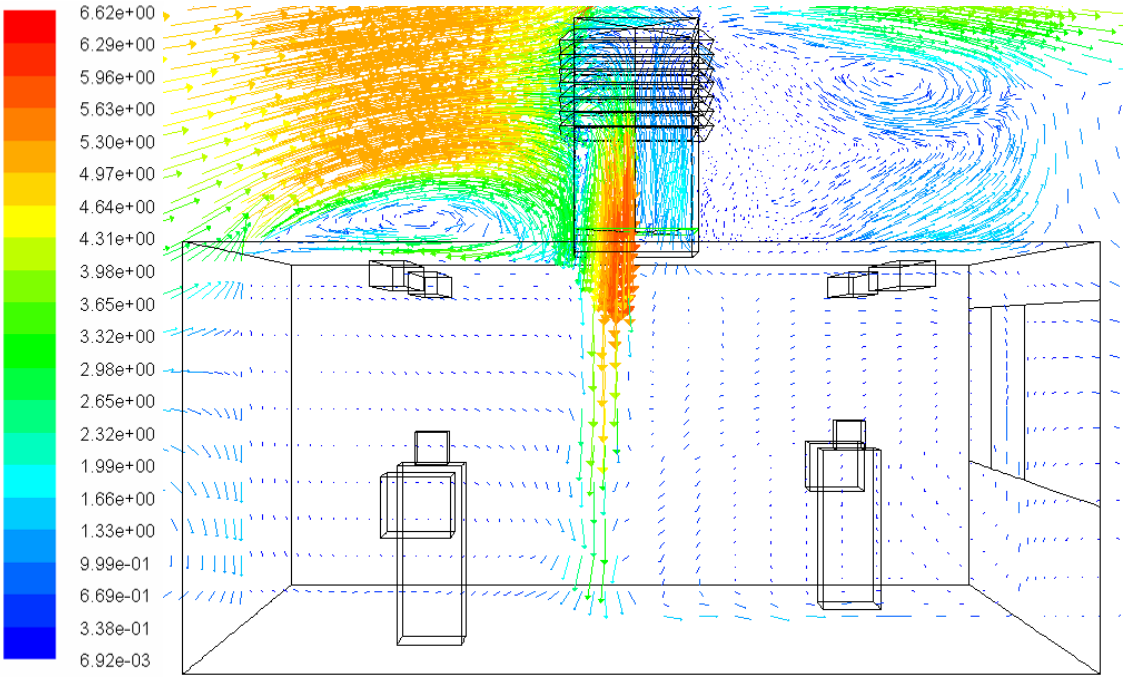
6.62e+00
6.29e+00
5.96e+00
5.63e+00
5.30e+00
4.97e+00
4.64e+00
4.31e+00
3.98e+00
3.65e+00
3.32e+00
2.98e+00
2.65e+00
2.32e+00
1.99e+00
1.66e+00
1.33e+00
9.99e-01
6.69e-01
3.38e-01
6.92e-03

(b)

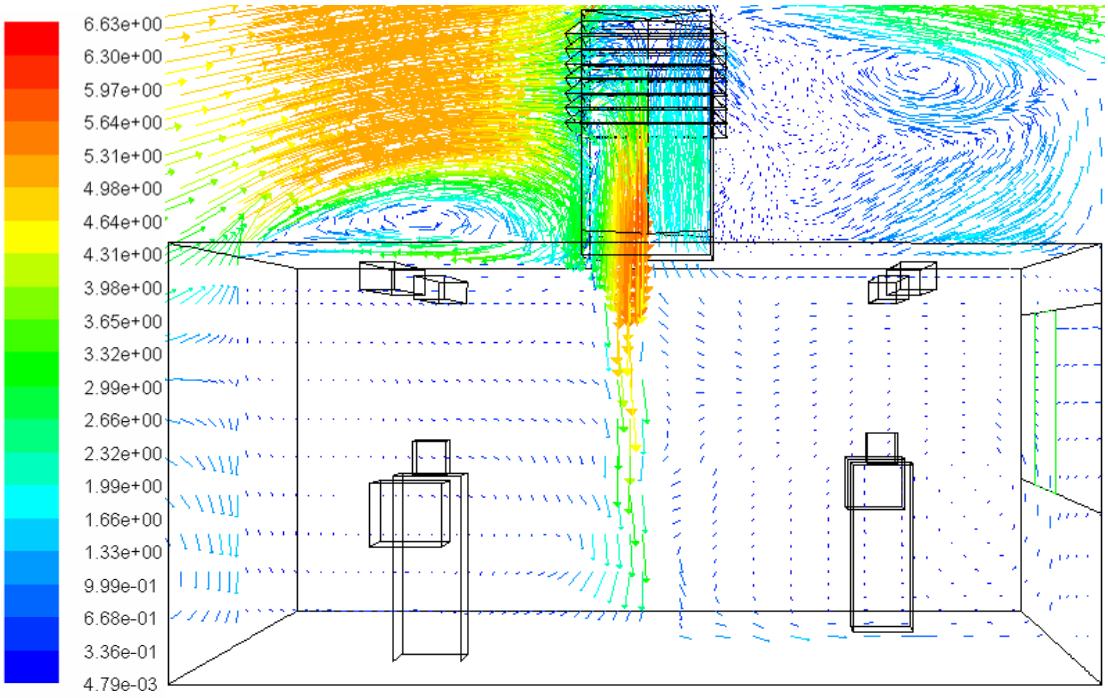

(c)

Figure 13 the velocity vector of the middle plane in the room model (a) without heat source and window; (b) with heat source and without window; (c) with heat source and the window located in the leeward wall

6.0 Results and Discussion

6.1 Wind Driven Simulations

The simulation results for wind driven models show an increase in internal velocities in proportion to an increased external velocity. This was as expected and is well documented in literature and previous wok by authors (10). The simulation models were run for a fixed external velocity of 10 m/s with an internal velocity measured at 780 L/sec. No internal heat sources were considered in this model.

Table 1 Simulation results of benchmark with counter-current flow

Velocity inlet speed (m/s)	Internal velocity (L/sec)
1	10
2	40
3	90
4	170
4.5	230
5	380
10	780

Table 2 Buoyancy CFD results

Velocity inlet speed (m/s)	Internal velocity (L/sec)	Case
10	420	No windows/No heat source
10	420	Heat source No window
10	625	Heat Source and Window

6.2 Buoyancy Simulations

The airflow rates of the three cases were compared in the figure 14.

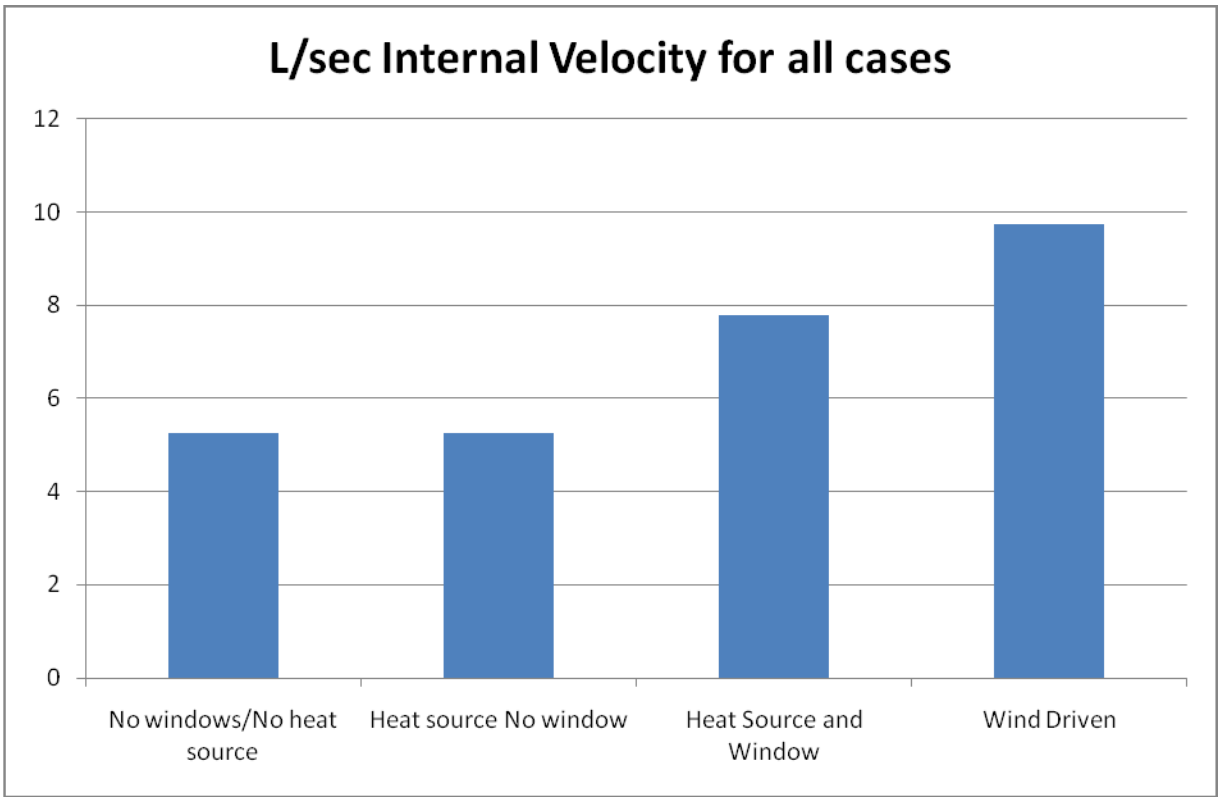

Figure 14 Internal velocity for normalised data

The airflow rates of case 1 and case 2 were almost the same, because of the little influence of the buoyancy effect. When the window was positioned on the leeward wall of the room, the airflow rate was increased by 47%. Except for the benefit of the wind catcher system, the other methods used together can much more enhance the ventilation performance.

In order to investigate the influence of the buoyancy effect on ventilation performance, the contours of velocity (three cases) and temperature (two cases) on the working plane were also shown in figure 15.

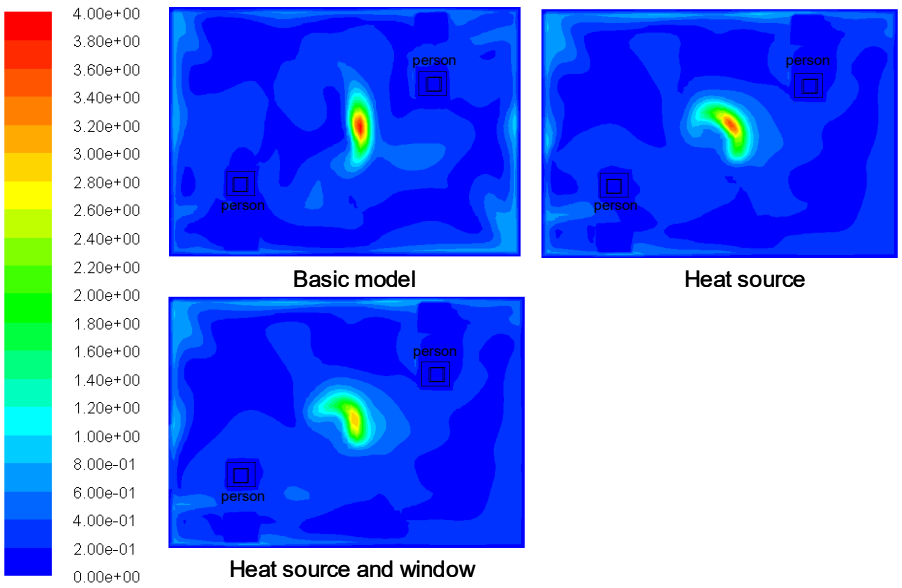

(a)

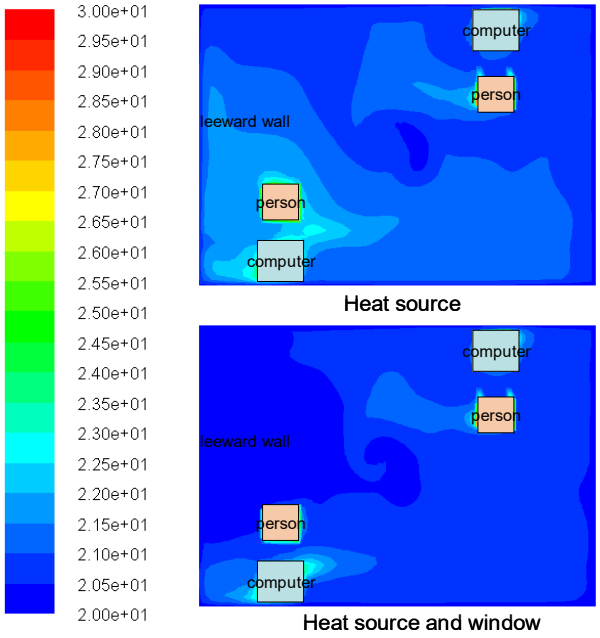

(b)

Figure 15 (a) velocity and (b) temperature distribution on the working plane

The velocity standard deviations on the working plane were 0.299 m/s (case 1), 0.303 m/s (case 2) and 0.280 m/s (case 3). The maximum velocity regions in the figure could also be seen in figure 13. The wind catcher system increased the uneven distribution of the velocity in the working plane, especially when there were heat sources. When there was a window on the leeward wall, the uniform of the velocity became better and the maximum of the velocity decreased in the middle of the office room. The temperature standard deviations on the working plane were 9.217 k (heat source) and 9.161 k (heat

source and window). Temperature distributions were shown in figure 15 (b). The window of the room made the temperature distribution more uniform. The half room of the windward direction was lower temperature than the other half in the heat source model without a window. Owing to the window on the leeward wall, the temperature of the half room in the leeward direction became lower.

6.3 Wind Driven Vs Buoyancy Simulations

In order to compare the two data sets they were both normalized against the internal volumes, thus the numbers became a trends rather than actual recorded data. The normalized data is presented in Table 3.

Table 3 Normalised data at 10 m/s for all cases

Case	L/Sec	Normalised Data (L/sec)
No windows/No heat source	420	5.25
Heat source No window	420	5.25
Heat Source and Window	625	7.8
Wind Driven	780	9.75

The effect of adding a heat source to the model was demonstrated to be insignificant, thus the heat alone will not provide the required buoyancy effect, moreover it must have an external outlet to create an effective airflow such as the addition of a window to the domain.

The effect of wind driven is shown to be 9.75 in comparison to 5.25 L/sec of the heat source only. This represents a 76% increase in internal velocity when using wind driven as opposed to buoyancy driven forces.

The effect of introducing a window into the buoyancy simulations increased the internal velocity to 7.8 L/sec. In comparison to the wind driven, it is again lower, with wind driven forces providing a further 28% increased internal velocity.

It should be noted that during the buoyancy simulations the effect of introducing a window increased the internal velocities by 47%, however the effect of introducing the wind driven force increased the internal velocity by 76%. Thus the effect of introducing a window to increase buoyancy is comparable to the wind driven force.

Conclusions

From the results it is concluded that the primary driving force for commercial wind tower's is externally driven wind, with the buoyancy effect as a secondary force. This study has quantified that in that wind driven provides 76% more internal ventilation than the buoyancy effects. Moreover this study determined that for the buoyancy to have any significant effect on the internal ventilation it requires an airflow passage other than that of the wind tower.

References

1 Transforming the market: Energy efficiency in buildings. World Business Council for Sustainable Development. April 2009.

2 Energy Efficiency and Renewable Energy. U.S Department of Energy. http://www1.eere.energy.gov/buildings/commercial/hvac.html Last accessed online (26/08/2009).

3 BRITISH STANDARDS INSTITUTION 1991. BS5925:1991: Ventilation principles and designing for natural ventilation. London, British Standards Institution.

4 HUGHES, B.R (2009). Performance Investigation of a Naturally Driven Building Ventilation Terminal. PhD, Sheffield Hallam University.

5 HUNT, G. R. and LINDEN, P. F. (1999). The fluid mechanics of natural ventilation - displacement ventilation by buoyancy - driven flows assisted by wind. *Building and environment,* **34** 707-720.

6 BUILDING SERVICES RESEARCH INFORMATION ASSOCIATION (2005). Wind-Driven Natural Ventilation Systems, A BSRIA Guide. Parker and teekaram.

7 ELMUALIM, Abbas A. (2006). Verification of design calculations of a wind Catcher/Tower natural ventilation system with performance testing in a real building. *International journal of ventilation,* **4** (4), 393-404.

8 ELMUALIM, Abbas A. a. e. a. u. (2006). Dynamic modelling of a wind catcher/tower turret for natural ventilation. *Building services engineering research and technology,* **27** (3), 165-182.

9 Liu, Li and MAK, C. M. (2007). The assessment of the performance of a windcatcher system using computational fluid dynamics. *Building and environment,* **42** (3), 1135-1141.

10 HUGHES, B. R. and GHANI, S. A. A. A. (2008). Investigation of a wind vent passive ventilation device against current fresh air supply recommendations. *Energy and buildings,* **40** (9), 1651-1659. .

11 HUGHES, B. R. and ABDUL GHANI, S. A. A. A.(2009). Numerical investigation into the effect of wind vent dampers on operating conditions. *Building and environment,* **44** (2), 237-248.

12 HUGHES, B. R. and ABDUL GHANI, S. A. A. A.(2009). A Numerical Investigation Into The Effect of Windvent Louvre External Angle On Passive Stack Ventilation Performance. *Building and Environment*, 45 (4) 1025-1036.

13 HUGHES, B.R and GHANI, S.A.A.A (2010) A Numerical Investigation Into The Feasibility Of A Passive-Assisted Natural Ventilation Device. International Journal Of Sustainable Energy. Article In Press [Available online 10.6/2010].

14 AYAD, Samir S. (1999). Computational study of natural ventilation. *Journal of wind engineering and industrial aerodynamics,* **82** (1-3), 49-68.

15 CHEN, Qingyan (. (2004). Using computational tools to factor wind into architectural environment design. *Energy and buildings,* **36** (12), 1197-1209.

16 EVOLA, G. and POPOV, V. (2006). Computational analysis of wind driven natural ventilation in buildings. *Energy and buildings,* **38** 491-501.

17 FLUENT. Fluent user manual 6.2(2003). *Fluent Incorporated.*

18 Department for Education and Skills Briefing framework for secondary school projects. Building Bulletin 98. April 1st 2004.

19 CHUNG, T. J. (2002). *Computational fluid dynamics.* Cambridge, University press.

20 JIANG, Y., ALLOCCA, C. and CHEN, Q. (2004). Validation of CFD simulations for natural ventilation. *International journal of ventilation,* **2** (4), 359-370.

21 HUGHES, B.R (2009). Performance Investigation of a Naturally Driven Building Ventilation Terminal. PhD, Sheffield Hallam University.

22 CHEN, Q. and SREBRIC, J. :. (2002). A procedure for verification, validation, and reporting of indoor environment CFD analyses. *HVAC&R research,* 8 (2), 201-216.

23 LIU, S. C. MAK, C. M. and NIU, J. L. (2011) Numerical evaluation of configuration and ventilation strategies for the windcatcher system. *Building and Environment*, article in press.